

# Intracellular $K^+$ Suppresses the Activation of Apoptosis in Lymphocytes\*

(Received for publication, June 26, 1997, and in revised form, September 4, 1997)

Francis M. Hughes, Jr., Carl D. Bortner, Geoffrey D. Purdy, and John A. Cidlowski‡

From the Laboratory of Signal Transduction, NIEHS, National Institutes of Health, Research Triangle Park, North Carolina 27709

Little is known about the mechanisms of suppression of apoptosis. We have addressed the novel possibility that the level of intracellular  $K^+$  regulates the apoptotic process by controlling the activity of death enzymes. We show that  $K^+$ , at normal intracellular levels, inhibits both apoptotic DNA fragmentation and caspase-3(CPP32)-like protease activation, suggesting that intracellular  $K^+$  loss must occur early during apoptosis. Direct measurement of  $K^+$  by inductively coupled plasma/mass spectrometry and flow cytometry indicates a major decrease in intracellular  $K^+$  concentration in the apoptotic cell. Flow cytometric analysis revealed that caspase and nuclease activity were restricted to the subpopulation of cells with reduced  $K^+$ . Disruption of the natural  $K^+$  electrochemical gradient suppressed the activity of both caspase and nuclease independent of the mode of activation of the apoptotic inducing agent, demonstrating that a decrease in intracellular  $K^+$  concentration is a necessary, early event in programmed cell death.

Apoptosis is a physiological form of cell death that occurs in response to a variety of signals. Although diverse agents induce apoptosis via unique signal transduction pathways, the process is remarkably similar in all systems. Morphologically, the cells in early stages of apoptosis shrink, and chromatin condenses. The nucleus then fragments, and the entire cell blebs into apoptotic bodies that maintain membrane integrity, ensuring encapsulation of the intracellular components. Genetic evidence has shown the requirement of specific gene products for the effective elimination of cells (1–3), although, in mammalian cells, the evidence suggests that these proteins are preformed in the nonapoptotic cell and maintained in an inactive state (4–9). Little is currently known about the mechanisms that provide this chronic suppressive effect on the apoptotic machinery.

In response to an apoptotic stimuli, there is a relief of the suppressive influences within a cell that manifests biochemical alterations including the activation of proteases and nucleases. Much attention has focused recently on the role of proteases related to interleukin-1 $\beta$  converting enzyme (recently renamed caspases (10)), and increases in caspase activity appear to be an early event in the common component of many apoptotic pathways (11–16). Caspases are synthesized and maintained in the cytoplasm as proenzymes which themselves must undergo a proteolytic activation, perhaps triggering apoptosis. The sub-

strates cleaved by these enzymes are numerous (17) and include both structural proteins (18–23) and enzymes (22, 24, 25). In addition to caspase activation, one or more nucleases are activated which destroy the genome through cleavage at specific structures (26–31). The active apoptotic nuclease(s) cleaves chromatin to produce nucleosomal (180–200 base pairs) or oligonucleosomal (multiples thereof) DNA fragments (32, 33). When analyzed by electrophoresis these fragments produce the widely recognized “apoptotic ladder.” Destruction of the structural proteins and the genome clearly represents a commitment step to the apoptotic process beyond which death is inevitable.

One of the most striking morphological changes common to all apoptotic cells is the loss of volume (*i.e.* cell shrinkage). Alterations in cell volume are typically mediated by changes in the intracellular ion levels, and apoptotic changes appear to be no exception (5, 34–36). However, nothing is known about the effects of these ionic changes on the activity of the underlying apoptotic machinery. Ions are well known to influence protein structure and can profoundly alter the activity of many different enzymes including proteases and nucleases (37–43). Since the majority of apoptotic enzyme activity takes place in a membrane-intact cell, one assumes that these enzymes should be functional in the presence of ion concentrations that approximate the intracellular environment.  $K^+$  is the predominant intracellular ion, and thus, we analyzed the effects of  $K^+$  on two key apoptotic enzymes, caspase-3-like protease and the internucleosomal DNA cleavage nuclease. The results demonstrate an *in vitro* inhibition of these enzymes by normal intracellular  $K^+$  concentrations and an *in vivo* association of  $K^+$  loss with their activation, implying the  $K^+$  efflux is necessary for the activation of apoptosis.

## EXPERIMENTAL PROCEDURES

### Preparation and Culture of Thymocytes

Thymocytes were prepared as described previously (5, 29, 35, 36, 44, 45). Briefly, bilaterally adrenalectomized adult male Sprague-Dawley rats were killed by decapitation and thymocytes quickly released by gentle homogenization. Cells were then filtered, washed, resuspended in PBS,<sup>1</sup> and counted on a hemacytometer. For normal cultures, cells were plated at  $5 \times 10^5$ /ml in normal medium (RPMI 1640 medium containing 10% heat-inactivated fetal calf serum (Intergen, Purchase, NY), 4 mM glutamine, 100 units/ml penicillin, 75 units/ml streptomycin sulfate and incubated at 37 °C in a 95% air, 5% CO<sub>2</sub> atmosphere).

### DNA Degradation Assays

**Autodigestion of Thymocyte Nuclei**—To investigate the spontaneous digestion of thymocyte nuclei, plasma membranes were lysed in ice-cold 10 mM MgCl<sub>2</sub>, 0.25% Nonidet P-40. Nuclei were pelleted and resus-

\* The costs of publication of this article were defrayed in part by the payment of page charges. This article must therefore be hereby marked “advertisement” in accordance with 18 U.S.C. Section 1734 solely to indicate this fact.

‡ To whom correspondence should be addressed: P. O. Box 12233; MD E2-02, Research Triangle Park, NC 27709. Tel.: 919-541-1564; Fax: 919-541-1367; E-mail: Cidlowski@niehs.nih.gov.

<sup>1</sup> The abbreviations used are: PBS, phosphate-buffered saline; DEX, dexamethasone; AFC, 7-amino-4-trifluoro-methylcoumarin; PBFI-AM, potassium-binding benzofuran isophthalate-acetoxymethylester; CHAPS, 3-[(3-cholamidopropyl)dimethylammonio]-1-propanesulfonic acid; [K]<sub>i</sub>, intracellular concentration of  $K^+$ .

pended in 50 mM Tris (pH 7.4), 2 mM  $\text{MgCl}_2$  at a concentration of  $4 \times 10^8$  nuclei/ml. Nuclei ( $4 \times 10^7$ ) were then added to microcentrifuge tubes containing final concentrations of 50 mM Tris (pH 7.4), 2 mM  $\text{MgCl}_2$ , 1 mM  $\text{CaCl}_2$ , and experimental treatments in a final volume of 400  $\mu\text{L}$ . Samples were rotated at room temperature for 1.5 h. Following incubation, 200  $\mu\text{L}$  were removed and EDTA, NaCl, and SDS added to 25 mM, 540 mM and 0.5%, respectively. TE buffer (10 mM Tris (pH 7.4), 1 mM EDTA) was added to bring the final volume up to 400  $\mu\text{L}$  and proteinase K added to 0.5 mg/ml, and the samples were incubated at 55 °C for 1 h prior to phenol/chloroform extraction and DNA precipitation. DNA was resuspended in 30  $\mu\text{L}$  of TE buffer (10  $\mu\text{g}$  of RNase A), and concentrations were determined spectrophotometrically after 16 h incubation (37 °C). DNA (15  $\mu\text{g}$ ) was electrophoresed (3.25 h, 80 V) through 1.8% agarose gels (20 mM Tris phosphate, 2 mM EDTA), stained with ethidium bromide, and photographed using UV transillumination. For quantitation, photographs were scanned (Silver Scanner III, La Cie Limited, Beaverton, OR) into a Macintosh computer, and densitometric plots were obtained using NIH Image software (NIH Bethesda, MD). The percent DNA degraded was calculated by dividing the low molecular weight area under the curve ( $<4.4$  kilobase pairs) by the total area and multiplying by 100.

**HeLa Nuclei Assay**—The HeLa nuclei assay was performed as described previously (29, 45, 46). Briefly, to prepare nuclear extracts nuclei were resuspended in 300 mM NaCl, 1 mM EDTA, 20 mM Tris (pH 7.4) and rotated for 1 h at 4 °C. Extracts were ultracentrifuged ( $165,000 \times g$ ; 1 h; 4 °C) and stored at  $-70$  °C. HeLa cells, grown in suspension culture, were counted, and nuclei were isolated as described above for thymocyte autodigestion. Nuclei were resuspended at  $2 \times 10^7$  nuclei/ml in 50 mM Tris (pH 7.4) and added ( $2 \times 10^6$  nuclei) to samples containing final concentrations of 50 mM Tris (pH 7.4), 2 mM  $\text{MgCl}_2$ , 1 mM  $\text{CaCl}_2$ , and experimental treatments in a total volume of 400  $\mu\text{L}$ . Following incubation for 5 h at room temperature with rotation, samples were processed for electrophoresis as described above for thymocyte autodigestion. In the absence of added extract, HeLa nuclei do not spontaneously degrade their DNA to any significant degree during the course of this incubation (29).

**Plasmid Degradation Assay**—One  $\mu\text{g}$  of linearized pUC18 plasmid was added to tubes containing 50 mM Tris, 1 mM  $\text{MgCl}_2$ , 1 mM  $\text{CaCl}_2$ , 10  $\mu\text{g}$  of thymocyte nuclear extract, and increasing concentrations of KCl. Samples were incubated for 5 h at 37 °C followed by the addition of 20  $\mu\text{g}$  of proteinase K, further incubation at 55 °C for 1 h, and electrophoresis for 1.5 h on a 1% agarose gel. DNA was visualized by ethidium bromide staining.

#### Measurement of Protease Activity

Caspase-1-like and caspase-3-like protease activity was measured using a fluorometric assay (47, 48). Briefly, cytoplasmic extracts were prepared by resuspending thymocytes ( $10^6/\text{ml}$ ) in 50 mM HEPES, 5 mM  $\text{MgCl}_2$ , 1 mM EGTA (pH 7.5) followed by Dounce homogenization. Alternatively, cells from culture were resuspended in 10 mM  $\text{MgCl}_2$ , 0.25% Nonidet P-40. Debris was pelleted at  $100,000 \times g$  for 30 min, and supernatants were placed on ice. In some experiments, extracts were next incubated for 1 h (30 °C) with 1 mM dATP and 10  $\mu\text{g}/\text{ml}$  cytochrome c. For caspase-3-like enzyme assays, 10–50  $\mu\text{g}$  of extract (measured by the method of Bradford (49)) was preincubated (10 mM dithiothreitol, 50 mM HEPES, 10% sucrose, 0.1% CHAPS (pH 7.5)  $\pm$  treatment) with 200  $\mu\text{M}$  of the noncompetitive inhibitor Z-DEVD-aldehyde (DEVD-al) (BaChem Biosciences, King of Prussia, PA) (1 h; 30 °C). Parallel samples were prepared without inhibitor. Substrate (Z-DEVD-AFC) (Kamiya Biomedical Co., Thousand Oaks, CA) was then added to all tubes (200  $\mu\text{M}$  final). Samples were incubated for (5 min; 30 °C), and their fluorescence at 505 nm was measured (excitation at 400 nm). Samples were incubated an additional hour and fluorescence again measured. A standard curve of fluorescence *versus* free AFC (Sigma) was used to calculate the specific activity of caspase-3-like enzymes in each sample. Caspase-1-like activity was measured in an identical manner using Z-YVAD-AFC (Kamiya Biomedical Co., Thousand Oaks, CA) as substrate and Z-YVAD-aldehyde (BaChem Biosciences, King of Prussia, PA) as inhibitor. Cleavage of caspase-3 was followed by *in vitro* translating caspase-3 (gene kindly provided by Dr. Vishva M. Dixit, University of Michigan Medical School, Ann Arbor) in the presence of Tran<sup>35</sup>S-label (ICN Pharmaceuticals, Costa Mesa, CA) using the TNT Coupled Reticulocyte Lysate System (Promega, Madison, WI) according to the recommendations of the manufacturer. *In vitro* translated product was then added (2.5  $\mu\text{L}/50$   $\mu\text{L}$  reaction volume) to the activation reactions described above. Following activation, samples were processed and analyzed by SDS-polyacrylamide gel electrophoresis followed by autoradiography.

#### Measurement of $[\text{K}^+]_i$

Following culture, cells were counted and sized on a Coulter Multi-sizer II (Coulter Corp., Hialeah, FL). Cells ( $2 \times 10^7$ ) were pelleted, washed in PBS, resuspended in 0.5 ml of PBS, and layered on top of a 0.5-ml oil (3:7, 1-bromododecane:1-bromododecane), 0.5-ml 15% trichloroacetic acid gradient and spun at  $\approx 14,000 \times g$  for 17 s.  $\text{K}^+$  in the trichloroacetic acid layer (intracellular  $\text{K}^+$ ) was measured by Inductively Coupled Plasma/Mass Spectrometry (Research Triangle Institute, Research Triangle, NC). Similar measurements were also obtained by atomic absorption.

#### Flow Cytometry

Intracellular  $\text{K}^+$  was measured by flow cytometry using the dye PBFI-AM (Molecular Probes, Eugene, OR) (50). Cells were loaded with PBFI-AM by addition of the dye to the media at a final concentration of 5  $\mu\text{M}$  for 1 h prior to harvest. After harvest, cells were resuspended in RPMI 1640 containing 10  $\mu\text{g}/\text{ml}$  propidium iodide. Analysis was accomplished using a Becton Dickinson FACStar flow cytometer (excitation 340–350 nm; emission 425 nm). For DNA content, cells were fixed in 70% ethanol, pelleted, washed once in PBS, and resuspended in PBS containing 20  $\mu\text{g}/\text{ml}$  propidium iodide. DNA content was then analyzed on a Becton Dickinson FACSsort flow cytometer. For caspase measurements, cells were sorted into normal sized and shrunken populations on a Becton Dickinson FACStar by gating on a dot plot of forward *versus* side scatter.

#### Culture of Thymocytes in High $\text{K}^+$ Medium

To assess the effects of  $\text{K}^+$ , we employed a culture system similar to that used by others (51). Thymocytes were cultured for 4 h in either normal or high  $\text{K}^+$  RPMI 1640 medium. Normal medium contains 5.3 mM KCl, 102.7 mM NaCl, whereas these concentrations were reversed in the high  $\text{K}^+$  medium. High  $\text{K}^+$  medium contains  $\text{Na}^+$  and  $\text{K}^+$  levels similar to intracellular levels while maintaining an isotonic environment (measured on a Wescor vapor pressure osmometer (Wescor, Logan, UT)). Fetal bovine serum used with the high  $\text{K}^+$  medium was previously dialyzed (molecular mass cutoff  $<3000$  kDa) against multiple changes of high  $\text{K}^+$  medium. Following incubation, cells were processed for DNA analysis or caspase-3-like activity.

#### Statistical Analysis of Results

Results were analyzed by Student's *t* test and considered significantly different from controls at  $p < 0.05$ .

#### RESULTS

**Intracellular Concentrations of KCl Inhibit Thymocyte Autodigestion *In Vitro***—Apoptotic DNA fragmentation can be recapitulated *in vitro* by incubation of isolated thymocyte nuclei with  $\text{Ca}^{2+}$  and  $\text{Mg}^{2+}$  in a process known as autodigestion. The nuclease is present within the nuclei in an inactive form, perhaps as a pro-enzyme, which is activated by the addition of  $\text{Ca}^{2+}$  and  $\text{Mg}^{2+}$ . When KCl was included in this incubation, DNA degradation was suppressed in a dose-dependent manner with a  $K_i \approx 70$  mM (Fig. 1). Inhibition was nearly complete at a  $\text{K}^+$  concentration equivalent to that normally found inside a cell (52). These data suggest that  $\text{K}^+$  efflux from an apoptotic cell is an important regulator of chromatin degradation. Interestingly, monovalent cations other than  $\text{K}^+$  ( $\text{Na}^+$ ,  $\text{Cs}^+$ ,  $\text{Cd}^+$ , and  $\text{Li}^+$ ) were also effective at similar concentrations. Moreover, identical results were seen when  $\text{Cl}^-$  was replaced with alternative anions ( $\text{H}_2\text{PO}_4^-$ ,  $\text{C}_2\text{H}_3\text{O}_2^-$ ). The similar effects of all these ions suggest that this response is not cation- or anion-specific but, rather, a result of the ionic strength of the buffer. The importance of  $\text{K}^+$  in nuclease inhibition *in vivo* lies in the fact that it is the only ion present at high concentrations within the cell. The results with  $\text{K}^+$  and other ions were not due to alterations in osmotic pressure since 300 mM mannitol (which exerts an osmotic pressure equivalent to 150 mM KCl) had no effect (data not shown).

**$\text{K}^+$  Directly Inhibits Active Nuclease *In Vitro***—The thymocyte autodigestion assay functionally consists of essentially two molecular events, activation of a latent nuclease and degradation of the chromatin substrate. To assess the effects of  $\text{K}^+$  on

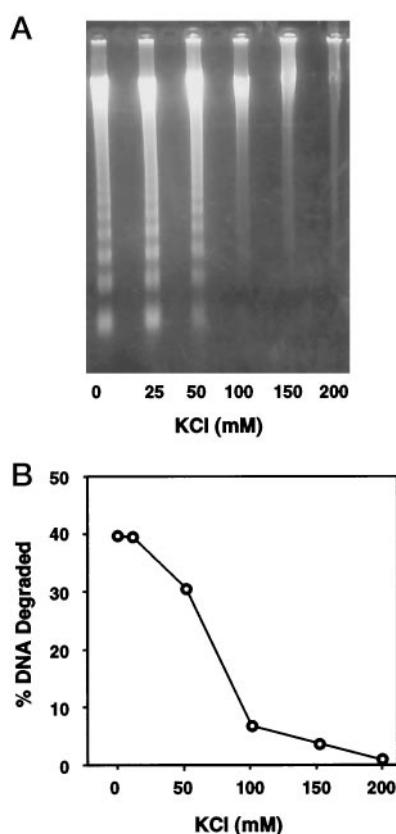


**FIG. 1. Increasing KCl concentrations suppress thymocyte autodigestion.** Thymocyte nuclei were prepared and incubated for 1.5 h in 50 mM Tris (pH 7.4), 2 mM  $\text{MgCl}_2$ , 1 mM  $\text{CaCl}_2$  containing increasing concentrations of KCl. Following incubation, thymocytes were processed and analyzed for DNA integrity. *A*, agarose gel demonstrating the inhibition of apoptotic-like internucleosomal DNA degradation by KCl. *B*, quantitation of the gel shown in *A* using densitometric analysis to graphically depict the loss of DNA degradation as a function of  $\text{K}^+$  concentration. The experiment was repeated three or more times with similar results.

active enzyme, we employed an *in vitro* apoptosis assay (29, 45, 46). In this assay, the apoptotic nuclease(s) is first activated in thymocytes *in vivo* by injection of the rat with the synthetic glucocorticoid dexamethasone (DEX). Active nuclease is then extracted from the thymocyte nuclei and applied to nuclei from healthy, growing HeLa cells that contain no capacity for autodigestion (29). In this assay (Fig. 2A), active nuclease was inhibited by  $\text{K}^+$  levels in a manner very similar to that seen in the autodigestion assays ( $K_i \approx 65$  mM).

Although intracellular levels of  $\text{K}^+$  clearly inhibit chromatin degradation by an active nuclease, it is possible that this effect is through a change in chromatin structure rather than a direct effect on the enzyme *per se*. To address this question we used linearized plasmid DNA as a substrate. As seen in Fig. 2B,  $\text{K}^+$  inhibited degradation of linearized pUC18 plasmid by thymocyte nuclear extracts in a dose-dependent manner ( $K_i \approx 80$  mM). Together, the results from these two independent assays demonstrate that  $\text{K}^+$  levels expected to be found in nondying cells exert a direct inhibitory effect on the active apoptotic nuclease and again imply that a decrease in  $[\text{K}^+]_i$  is a prerequisite for apoptotic DNA degradation.

**$\text{K}^+$  Inhibits the Activation of Pro-caspase-3 but Not the Activity of Mature Caspase-3**—Activation of caspases is a central event that occurs upstream of DNA fragmentation during apoptosis. To establish the extent of  $\text{K}^+$  effects on the apoptotic machinery, we assessed the effects of  $\text{K}^+$  on caspase activity. Fig. 3A demonstrates that caspase-1-like activity (enzyme ac-

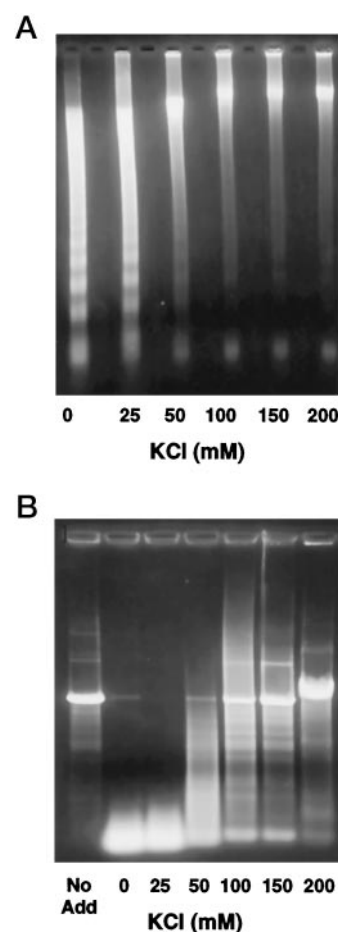


**FIG. 2. KCl directly suppresses active nuclease in a dose-dependent manner.** Nuclease activity extracted from thymocytes treated with DEX *in vivo* for 4 h was analyzed in two separate assays for the inhibitory effects of KCl. *A*, HeLa nuclei assay: agarose gel depicting the integrity of HeLa chromatin after incubation (5 h) with 100  $\mu\text{g}$  of thymocyte nuclear extract. Following incubation, DNA was extracted and prepared as described under "Experimental Procedures." This experiment has been repeated three or more times with similar results. *B*, plasmid degradation assay: agarose gel depicting the integrity of linearized pUC18 plasmid after incubation with thymocyte nuclear extract (10  $\mu\text{g}$ ) and increasing concentrations of KCl for 5 h. The *No Add* depicts samples treated exactly as the others without any added thymocyte extract.

tivity that is inhibited by Z-YVAD-al) remains low in extracts prepared from thymocytes treated with dexamethasone *in vivo* for 4 h (DEX), similar to extracts from untreated animals (CON). However, caspase-3-like activity (protease activity(ies) inhibited by Z-DEVD-al) is increased 9-fold in these same cytoplasmic extracts (Fig. 3B), suggesting that caspase-3-like enzymes may play a predominant role, relative to caspase-1-like enzymes, in DEX-induced rat thymocyte apoptosis. This result is consistent with other studies (53, 54). Fig. 3C demonstrates that extracts from untreated thymocytes also contain pro-caspase-3-like enzymes that can be activated by preincubation for 1 h (30  $^{\circ}\text{C}$ ) with 1 mM dATP and 10  $\mu\text{g}/\text{ml}$  cytochrome *c*, similar to that seen with other cells (55). Thus, the increase in caspase-3-like activity seen in Fig. 3B is not due to an inability to extract protease from nondying cells. The greatly increased activity in the dATP and cytochrome *c*-activated extracts, compared with that present in extracts from thymocytes treated *in vivo* with dexamethasone, probably reflects the heterogeneous response to the steroid *in vivo* compared with the homogeneous activation accomplished *in vitro* with dATP and cytochrome *c*. More importantly, these results allow us to dis-



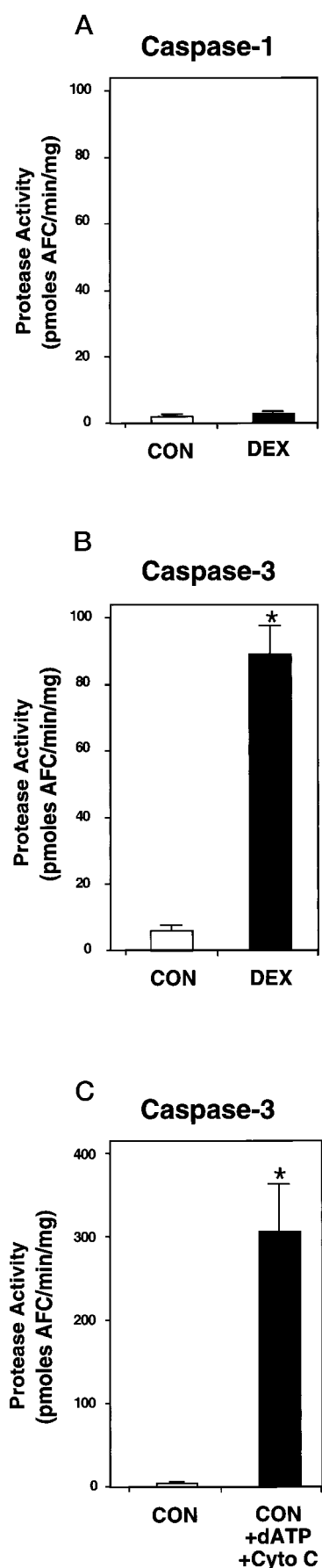


FIG. 3. **Caspase activity graphs.** Cytoplasmic extracts were prepared from thymocytes isolated from untreated (CON) or 4 h *in vivo* DEX-treated (DEX) rats and analyzed for caspase activity based on

tinguish between the effects of  $K^+$  on the activity of mature caspase-3-like enzymes *versus* the activation of the proenzyme molecule.

The effects of  $K^+$  on mature caspase-3-like activity was assessed using cytoplasmic extracts from thymocytes treated with dexamethasone *in vivo*. When  $K^+$  in the enzyme assay was varied from 0 to 200 mM, these levels had no effect on the activity of the active protease (Fig. 4A). Similarly, *in vitro*-activated caspase-3-like enzymes (*i.e.* extracts from untreated rats that had been previously activated *in vitro* by dATP and cytochrome *c*) were refractory to any inhibitory effects of  $K^+$  (Fig. 4D). To assess the effects of  $K^+$  on activation of the pro-enzyme, we incubated the extracts from untreated animals with dATP and cytochrome *c* for 1 h in the presence of increasing concentrations of KCl. As shown in Fig. 4B,  $K^+$  inhibited the *in vitro* activation of caspase-3-like enzymes in a dose-dependent manner ( $K_i \approx 40$  mM) with nearly complete suppression by 100 mM KCl. Thus, physiological concentrations of  $K^+$ , expected to be found in nonapoptotic cells, can directly inhibit the activation of pro-caspase-3-like enzymes. Since the inhibitor used is likely to block the activity of several caspases, we sought to determine the specificity of  $K^+$  inhibition by evaluating the selective cleavage of pro-caspase-3 to its active subunits. Fig. 3C shows that dATP and cytochrome *c* stimulate cleavage of the 32-kDa *in vitro* transcribed/translated  $^{35}S$ -pro-caspase-3 molecule into both the 17/11-kDa and 20/11-kDa subunits. Thus, at least one target of  $K^+$  inhibition is caspase-3 itself occurring at the level of the cleavage reaction. Together, these data demonstrate that  $K^+$  levels found in non-apoptotic cells are sufficient to inhibit activation of caspase-3-like enzymes *in vitro*.

**Kinetic Analysis of Viability, Caspase-3-like Activity, DNA Degradation, and  $[K^+]_i$  during Apoptosis *in Vivo***—The data have suggested that the intracellular  $K^+$  concentration must decrease within cells signaled to undergo apoptosis. Using inductively coupled plasma/mass spectrometry, we analyzed the relationship between intracellular  $K^+$  levels and other features of apoptosis. As shown in Fig. 5A, viability remains >93% in this experiment, obviating any concerns with membrane integrity. As hypothesized, the average  $[K^+]_i$  decreased in the dying thymocyte population (Fig. 5B) with a significant shift first detected after 4 h and a steady decrease thereafter to 56 mM at 8 h. Thus, the  $[K^+]_i$  in an apoptotic cell decreased to a level sufficient for enzyme activation. It should be noted, however, that these data represent the average  $[K^+]_i$  in the entire population of cells asynchronously undergoing apoptosis (56). Therefore, this reduction in  $[K^+]_i$  may not accurately reflect the magnitude of change that occurs within a single apoptotic cell. Previous estimates from our lab have placed the  $[K^+]_i$  in the shrunken apoptotic cells at  $\approx 35$  mM (56). Analysis of chromatin integrity (Fig. 5C) revealed the appearance of oligonucleosomal fragments after 4 h, the intensity of which continued to increase. Similarly, caspase-3-like activity (Fig. 5D) increased in a time-dependent manner with a significant increase detected as early as 2 h. The appearance of caspase activity prior to

their ability to cleave specific fluorogenic substrates. Asterisks indicate a significant difference from control extracts ( $p < 0.05$ ). A, caspase-1-like activity (Z-YVAD-AFC-cleavable activity) in CON and DEX extracts. Results are presented as the mean  $\pm$  S.E. of three separate experiments. B, caspase-3-like activity (Z-DEVD-AFC-cleavable activity) in CON and DEX extracts. Results are presented as the mean  $\pm$  S.E. of three separate experiments. C, activation of pro-caspase-3-like activity in CON extracts by preincubation for 1 h (30 °C) with 1 mM dATP and 10  $\mu$ g/ml cytochrome *c*. Following this preincubation, samples were immediately analyzed in the caspase-3 assay for the ability to cleave Z-DEVD-AFC. Results are presented as the mean  $\pm$  S.E. of four separate experiments.

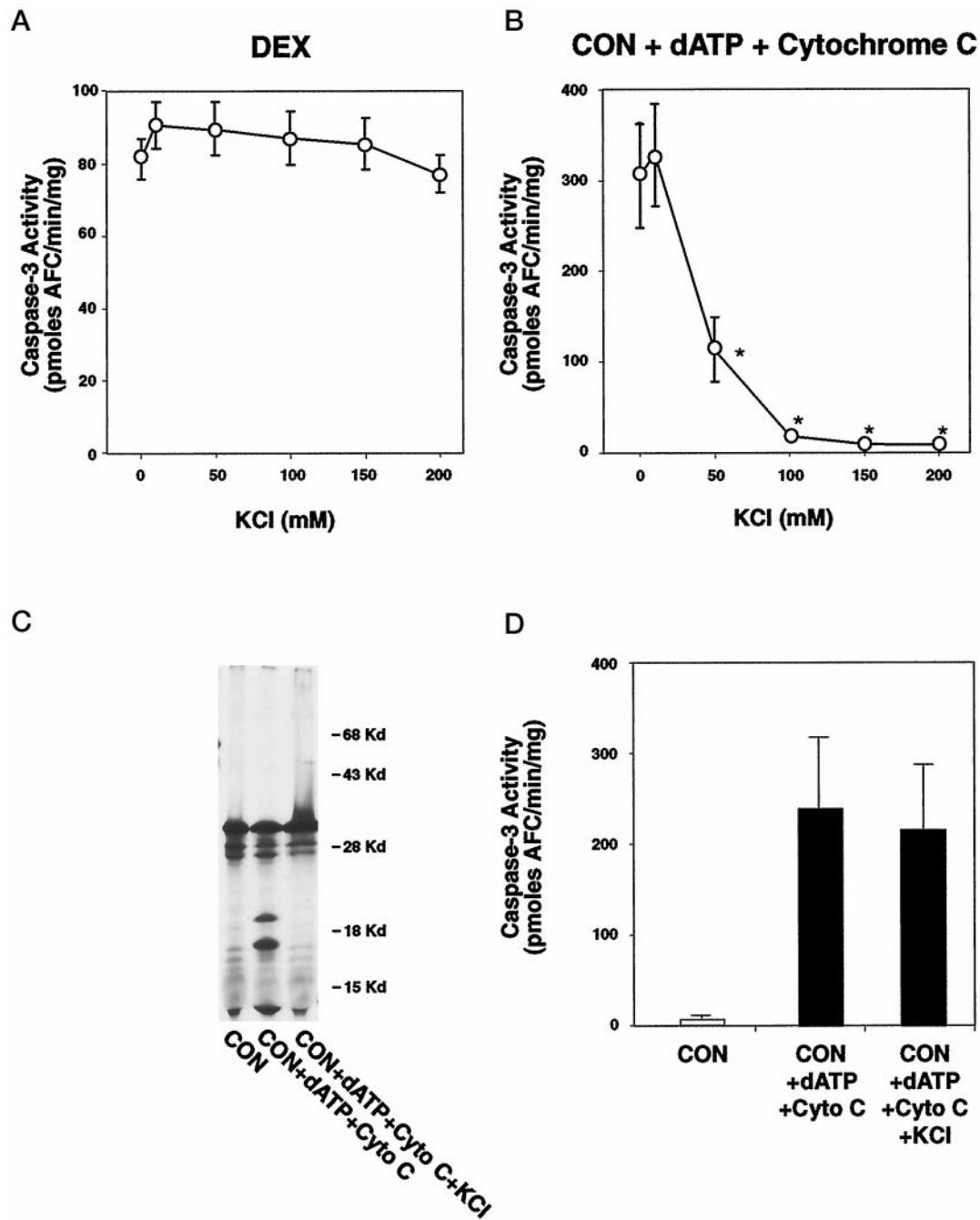
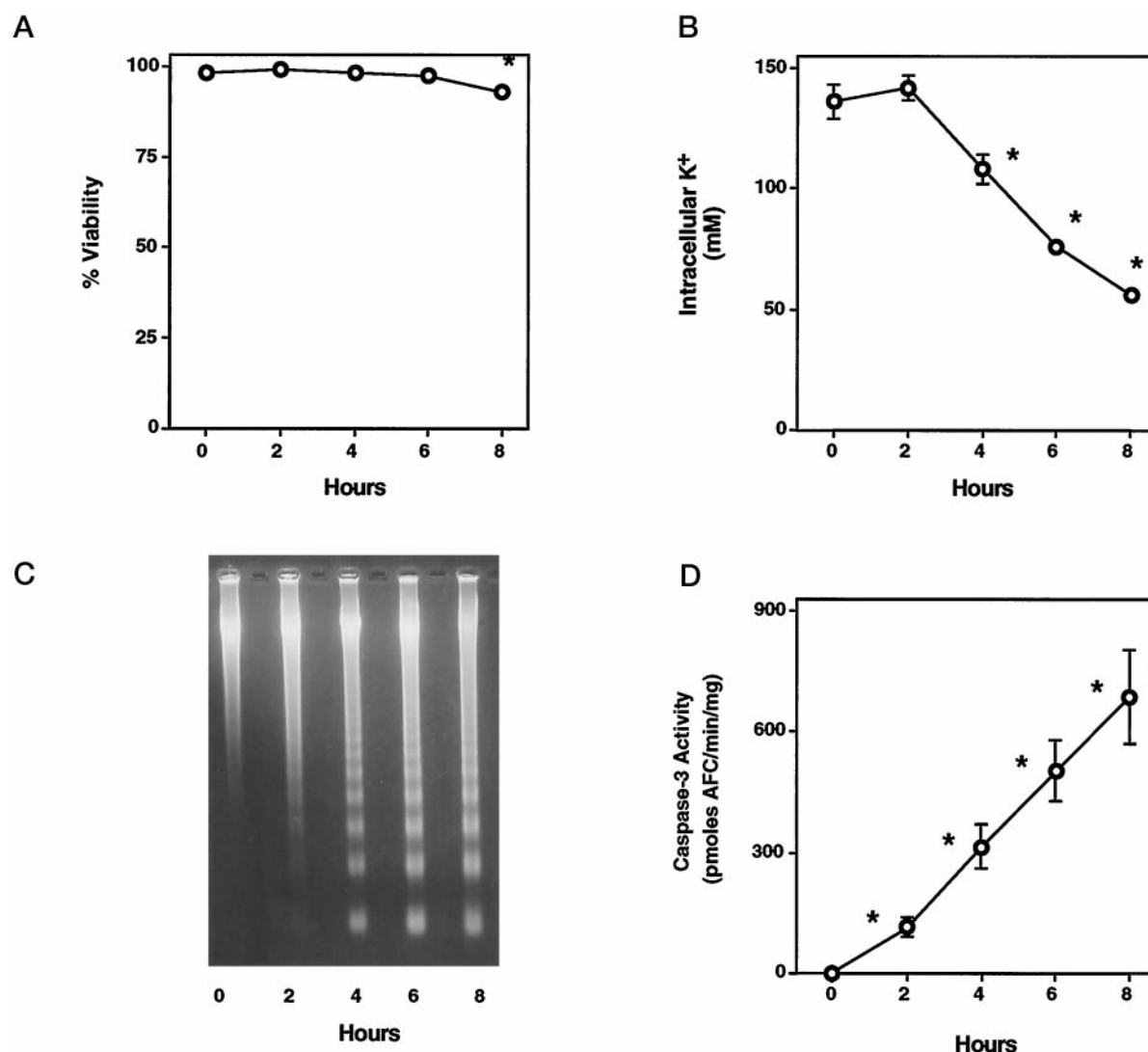


FIG. 4. Effects of increasing concentrations of  $K^+$  on caspase-3-like activity (A) and the activation of pro-caspase-3-like enzymes by dATP and cytochrome *c* (B). A, DEX extracts, identical to those used in Fig. 3, were analyzed for caspase-3-like activity in the presence of increasing concentrations of KCl. Results represent the mean  $\pm$  S.E. from three independent experiments. B, CON extracts, identical to those used in Fig. 3, were incubated 1 h (30 °C) with 1 mM dATP, 10  $\mu$ g/ml cytochrome *c*, and increasing concentrations of KCl. Immediately following this incubation, extracts were analyzed in the caspase-3-like enzyme assay. Results are the mean  $\pm$  S.E. from four separate experiments. Asterisks indicate a significant difference from the 0 mM KCl controls ( $p < 0.05$ ). C, CON extracts were activated in a manner identical to B with the inclusion of 2.5  $\mu$ l  $^{35}$ S-caspase-3. Samples were then processed for SDS-polyacrylamide gel electrophoresis and analyzed by autoradiography. D, CON extracts, identical to those used above, were tested directly (CON) or first incubated 1 h (30 °C) with 1 mM dATP and 10  $\mu$ g of cytochrome *c* before being analyzed in the caspase-3-like enzyme assay. The caspase-3-like enzyme assay was then performed in the absence (CON and CON + dATP + Cyto *C*) or presence (CON + dATP + Cyto *C* + KCl) of 150 mM KCl. The results are reported as the mean  $\pm$  S.E. of four separate experiments.

detection of a decrease in  $[K^+]_i$ , seemed paradoxical in light of the  $K_i$  for inhibition of activation of caspase-3-like enzymes. Thus we analyzed  $K^+$ , caspase, and nuclease activities in the normal-sized and shrunken cells to determine if specific subpopulations were responsible for the detection of protease activity at 2 h.

**Caspase and Nuclease Activity Is Restricted to Cells with Lowered Intracellular  $K^+$  Levels in Vivo**—As previously shown, apoptosis proceeds asynchronously (56), forming two distinct

subpopulations that can be defined by the flow cytometer based on forward light scattering properties (Fig. 6A) (5). By sorting these subpopulations, assessing cell size, and comparing to freshly isolated (nondying) thymocytes, we have ascertained that they are “normal” sized ( $106.6 \pm 0.9$  fl) and “shrunken” ( $71.0 \pm 5.1$  fl) subpopulations, respectively (Fig. 6A). Extrusion of  $K^+$  has been suggested to mediate the loss of volume during apoptosis (5, 35, 36, 57), and so we analyzed  $K^+$  levels in these subpopulations with the intracellular  $K^+$  dye PBFI-AM (Mo-



**FIG. 5. Time course of DEX-induced apoptosis in rat thymocytes *in vitro*.** Thymocytes were placed in culture ( $5 \times 10^6/\text{ml}$ ) in the presence of  $1 \mu\text{M}$  DEX and harvested every 2 h. Viability, intracellular  $\text{K}^+$ , DNA fragmentation, and caspase-3-like activity was then assessed. Individual points were repeated 4–10 times, and the results (in A, B, and D) are presented as the mean  $\pm$  S.E. of all measurements. Asterisks indicate a significant difference from the appropriate 0 h control ( $p < 0.05$ ). Error bars not apparent are contained within the symbol. A, cell viability over time, as determined by trypan blue staining. B, average concentration of intracellular  $\text{K}^+$  ( $[\text{K}^+]_i$ ) in the culture population. C, agarose gel showing the integrity of DNA in these cultures. D, caspase-3-like activity.

lecular Probes, Eugene, OR) (50). Because the 2-h time point in Fig. 5 had appeared paradoxical, we choose this time point to examine. As shown in Fig. 6A, a small subpopulation of shrunken cells had formed by 2 h of culture that was absent in the freshly isolated cells (fresh data not shown). Interestingly, as shown in Fig. 6B, the PBFI-AM ( $\text{K}^+$ ) fluorescence decreased  $>95\%$  in the shrunken population relative to the normal sized cells, demonstrating that lowered  $\text{K}^+$  levels are restricted to the shrunken subpopulation of thymocytes. Although PBFI-AM measures  $\text{K}^+$  content, two lines of evidence suggest that the decrease in fluorescence reflects a significant decrease in the intracellular concentration of this cation. First, we measured a 60% decrease in the average  $[\text{K}^+]_i$  in the entire DEX-treated population over time (Fig. 5B). However, PBFI fluorescence in the normal sized subpopulation within these cultures was identical to the PBFI fluorescence in the freshly isolated (nondying) population (data not shown), suggesting that the normal sized subpopulation has a normal  $[\text{K}^+]_i$ . Thus, the measured decrease in  $[\text{K}^+]_i$  in the entire population is likely to arise from a large decrease in  $[\text{K}^+]_i$  in the shrunken population. Second, the 95% loss in PBFI-AM fluorescence in the shrunken

subpopulation is correlated with only a 33% loss of volume (from above normal cells are  $106.6 \pm 0.9 \text{ fl}$  and shrunken cells  $71.0 \pm 5.1 \text{ fl}$ ). This large change in fluorescence with only a small change in size is again suggestive of a significant decrease in  $[\text{K}^+]_i$  in the shrunken cells.

The normal and shrunken subpopulations were next analyzed for their DNA content by flow cytometry using an established measure of chromatin degradation at the single cell level. As shown in Fig. 6C, normal sized cells produce a typical cell cycle histogram with the vast majority of cells being diploid (fluorescing at  $\approx 230$  units) and a small amount present in the S and  $\text{G}_2/\text{M}$  phases. In contrast, the shrunken subpopulation displayed only a subdiploid (apoptotic) amount of DNA, demonstrating a strong correlation between a reduction in intracellular  $\text{K}^+$  and nuclease activation in thymocytes. Finally, we examined the caspase-3-like activity present in the normal and shrunken cells in these two populations. Similar to the DNA fragmentation results, Fig. 6D demonstrates that the vast majority of caspase-3 activity is restricted to the shrunken population (Fig. 6D). Thus, by examining subpopulations of cells, we

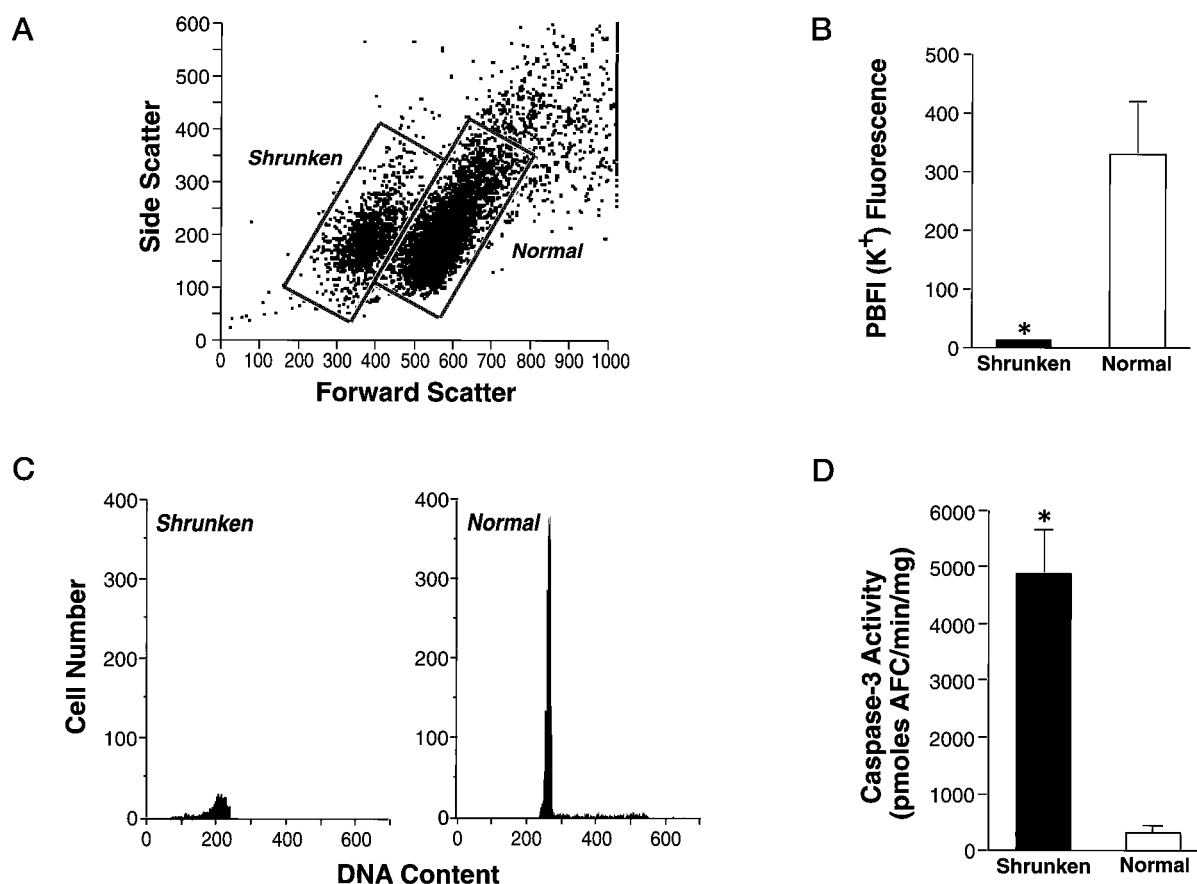


**FIG. 6. Caspase and nuclease activity is restricted to cells with lowered intracellular  $K^+$ .** Thymocytes were plated in culture ( $5 \times 10^6$ /ml) in the presence of  $1 \mu M$  DEX for 2 h. An aliquot of cells were fixed in 70% ethanol for >18 h prior to staining with propidium iodide and analysis of cell size and DNA content. For  $K^+$  measurements, cells were loaded for 1 h with  $5 \mu M$  PBFI-AM prior to analysis. For caspase activity, cells were sorted (Becton Dickinson FACStar) and processed as described under "Experimental Procedures." **A**, dot plot showing the size distribution of thymocytes (forward light scatter versus side light scatter) into two distinct subpopulations. **B**, PBFI-AM fluorescence associated with the normal sized and shrunken subpopulations. **C**, DNA histograms showing the DNA content of the normal sized and shrunken subpopulations. **D**, caspase-3-like activity extracted from normal sized and shrunken thymocytes. The results in **B** and **D** are the mean  $\pm$  S.E. from three separate sorting experiments. The asterisks indicate a significant difference from the normal population. The results in **A** and **C** are from a representative experiment repeated two additional times with similar results.

have shown a strict association of cell shrinkage with intracellular  $K^+$  loss and demonstrated that only those cells that have decreased intracellular  $K^+$  possess degraded DNA and caspase-3 activity. Coupled with the *in vitro* data in Figs. 1–4, the data strongly suggest that a decrease in  $[K^+]_i$  is not only associated with apoptosis but is a necessary component of the process.

**DNA Degradation and Caspase-3-like Enzyme Activation in Vivo Is Suppressed by High Extracellular  $K^+$** —To test the hypothesis that this loss of  $K^+$  is necessary for the progression of apoptosis, we suppressed  $K^+$  efflux by treating cells in medium containing high  $K^+$  levels ( $K^+$  medium) (51, 58). In this medium the concentration of  $Na^+$  has been reduced to preserve isotonic properties. As shown in Fig. 7, culture in this medium completely inhibited DNA fragmentation in thymocytes in response to three separate apoptotic agents (dexamethasone, thapsigargin, and staurosporin) that initiate apoptosis by three independent mechanisms. The effects on caspase-3-like enzyme activation paralleled the effects on DNA cleavage demonstrating a general (not signal-dependent) inhibitory influence of  $K^+$  on the apoptotic machinery. The caspase-3-like activity detected in cells cultured in  $K^+$  medium is equal to that observed in thymocytes cultured in normal or  $K^+$  medium in the absence of apoptotic stimuli (data not shown). Together, the results indicate that the inhibitory effects of  $K^+$  are independent of the apoptotic stimulus and suggest that  $K^+$  loss early in

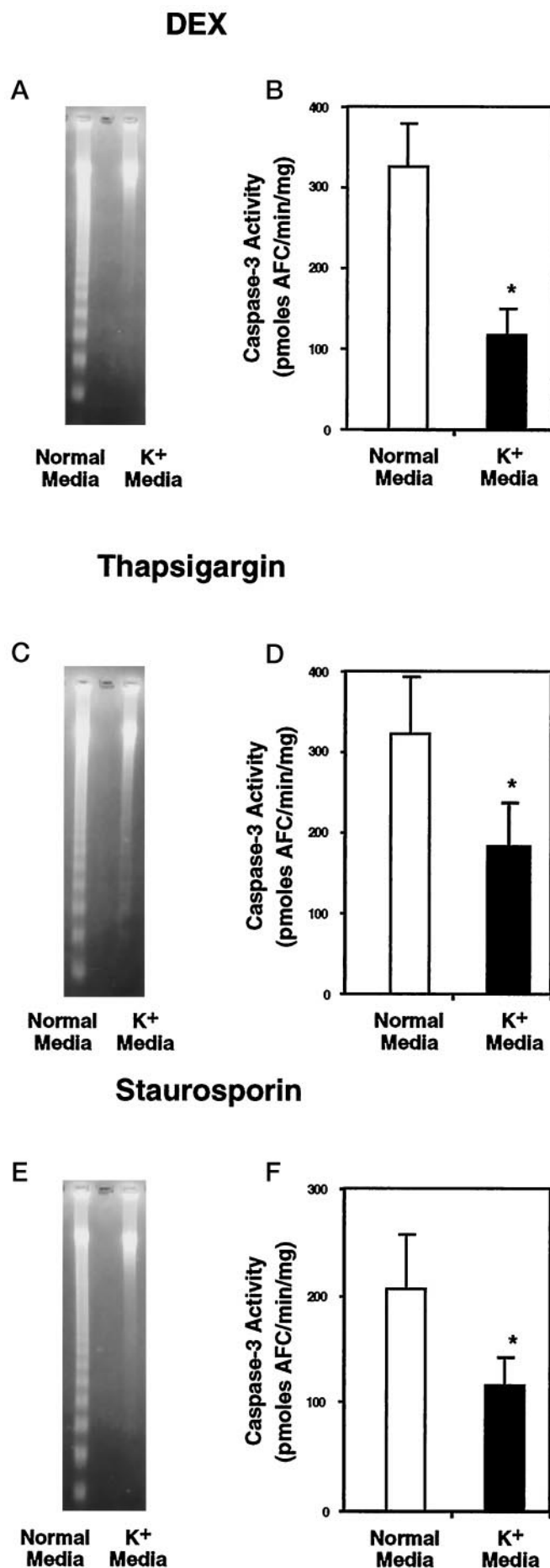
apoptosis is a necessary requirement for progression of the death program.

#### DISCUSSION

Apoptosis can be activated in a variety of cells through diverse signaling pathways. However, all apoptotic insults result in a highly conserved series of morphological and biochemical changes, suggesting a common pathway distal to cell and/or signal-specific events. Apoptotic cells display a significant cell shrinkage, and  $K^+$  efflux has been suggested to mediate this loss of volume (5, 35, 36, 57). Our initial results demonstrating that  $K^+$  is inhibitory to apoptotic nuclease activity focused our attention on the potential role of this ion as a central regulator of the apoptotic machinery. Further experiments demonstrated a direct effect of  $K^+$  on the active nuclease and show that the effect is a result of ionic strength. Thus, the importance of  $K^+$  to apoptotic nuclease activity lies in the fact that it is normally present within a cell in inhibitory concentrations and therefore is in position to apply a tonic suppressive force on the nuclease.

We extended these studies to earlier apoptotic enzymes (caspases) that function upstream of DNA fragmentation and found that activation of caspase-3-like proteases is also inhibited by physiological levels of  $K^+$ , and this inhibition occurs at the level of cleavage of the pro-enzyme. Interestingly, caspase activity and DNA fragmentation were restricted to a subpopu-





lation of cells that contained a lower K<sup>+</sup> level, suggesting that cell shrinkage and K<sup>+</sup> efflux must occur before the enzymes become functional. Finally, DNA fragmentation and pro-caspase-3-like enzyme activation was suppressed within several apoptotic populations by disrupting the normal electrochemical gradient of K<sup>+</sup> and, therefore, preventing K<sup>+</sup> efflux. Together, these results demonstrate an inhibitory effect of K<sup>+</sup> on two major enzymes common to many models of apoptosis and suggest that K<sup>+</sup> efflux plays a critical role in the apoptotic process.

Although a decrease in [K<sup>+</sup>]<sub>i</sub> is a prerequisite event during apoptosis, it is not a trigger for activation of caspase-3-like enzymes or the internucleosomal cleavage enzyme. For example, the internucleosomal cleavage enzyme is constitutively expressed in normal thymocytes but is maintained in an inactive conformation (46). Placing the inactive nuclease in K<sup>+</sup>-deficient buffer is not sufficient to activate its DNA degrading properties, although it may be activated by other methods (46). Similarly, incubation of pro-caspase-3-like enzymes in low K<sup>+</sup> buffer (in the absence of dATP and cytochrome *c*) was ineffective in activating the enzyme. Thus, both enzymes require separate apoptotic activating signals, whereas high [K<sup>+</sup>]<sub>i</sub> acts as an early checkpoint to suppress inappropriate activation of these enzymes.

The inhibitory effects of K<sup>+</sup> on caspase activity likely includes other members of the caspase family. Walev *et al.* (51) measured a significant shift from mature interleukin-1 $\beta$  toward pro-interleukin-1 $\beta$  secretion when monocytes were cultured in K<sup>+</sup> medium (similar to Fig. 7). Likewise, Perregaux *et al.* (59) recently demonstrated that reducing intracellular K<sup>+</sup> enhanced mature interleukin-1 $\beta$  secretion while increasing intracellular K<sup>+</sup> shifted production toward the pro-cytokine form. The present results with caspase-3-like enzymes, together with these reports on caspase-1, suggest that inhibition by K<sup>+</sup> may be a general post-translational regulatory property of this class of proteases. To our knowledge, this is the first study to document the inhibitory effects of K<sup>+</sup> on apoptotic enzyme activity, although K<sup>+</sup> loss from an apoptotic cell has been proposed as a mechanism of cells shrinkage (5, 34–36). Interestingly, Barbiero *et al.* (35) measured K<sup>+</sup> levels during apoptosis in a fibroblast cell line (L-cells) and reported that the average intracellular concentration fell to 50 mM, a number consistent with our measurement of 56 mM (Fig. 6). We have shown that the presence of volume regulatory mechanisms that increase intracellular K<sup>+</sup> inhibits apoptosis, suggesting these mechanisms must be overridden to initiate the apoptotic cascade (5). The present study, however, provides a critical role for K<sup>+</sup> loss in the control of enzymatic activity.

The mechanisms that drive the apoptotic decrease in intracellular K<sup>+</sup> are presently unknown but likely involve some aspect of normal cell volume control mechanisms. For example, when placed in a hypotonic environment, cells initially swell due to the uptake of water. This increase in cell volume acti-

**Fig. 7. The effects of K<sup>+</sup> media on DNA integrity and caspase-3-like activity in rat thymocytes in response to several apoptosis-inducing agents.** Thymocytes were cultured ( $5 \times 10^5$ /ml) in normal media or K<sup>+</sup> media for 4 h in the presence of 1  $\mu$ M DEX (A and B), 2  $\mu$ M Thapsigargin, or 100 nM Staurosporin before the cells were harvested and analyzed for DNA integrity and caspase-3-like activity. A, agarose gel comparing DNA integrity in cells incubated in normal media and K<sup>+</sup> media in the presence of 1  $\mu$ M DEX. B, caspase-3-like activity extracted from cells incubated as in A. C, agarose gel comparing DNA integrity in cells incubated in normal media and K<sup>+</sup> media in the presence of 2  $\mu$ M thapsigargin. D, caspase-3-like activity extracted from cells incubated as in C. E, agarose gel comparing DNA integrity in cells incubated in normal media and K<sup>+</sup> media in the presence of 100 nM staurosporin. F, caspase-3-like activity extracted from cells incubated as in E.



vates a process known as a regulatory volume decrease in which  $K^+$  efflux draws water out of the cell and returns the cell to a near-normal size (60–62). In lymphocytes, this process is mediated through quinine-sensitive  $K^+$  channels that allow efflux of  $K^+$  down its concentration gradient (63, 64). It is possible that a similar mechanism becomes activated during apoptosis, for when the electrochemical gradient of  $K^+$  is abolished in the present study, DNA degradation and caspase-3-like enzyme activation are suppressed (Fig. 7). We have not, however, been able to block apoptosis or cell shrinkage with quinine,<sup>2</sup> implying that different  $K^+$  channels or transport pathways are involved in cell shrinkage during apoptosis. The exact channel(s) responsible for extrusion of  $K^+$  during apoptosis is the focus of our ongoing research.

The results of our study indicate that the ionic strength of the intracellular compartment functions to maintain apoptotic systems in an inactive state. In most cells  $K^+$  is the major contributor to this ionic strength, although  $Na^+$  levels should not be disregarded in light of our findings that high  $Na^+$  levels can inhibit DNA degradation. Since normal intracellular  $Na^+$  levels are typically an order of magnitude lower than  $K^+$  levels, they probably contribute only a small amount to the resting intracellular ionic strength. Given the large reduction in  $K^+$  one might predict that  $Na^+$  would increase as  $K^+$  decreases. However, we have recently found that  $Na^+$  levels actually decrease during apoptosis (65), suggesting that  $Na^+$  does not significantly influence the  $K^+$ -mediated changes in intracellular ionic strength during apoptosis.

It is interesting that the apoptosis inhibitor Bcl-x<sub>L</sub>, a molecule related to Bcl-2, has recently been shown to form a three-dimensional structure similar to the pore-forming domains of bacterial toxins (66). Moreover, this molecule forms cation-selective pores in synthetic lipid membranes at physiological pH, and these pores are capable of conducting a  $K^+$  current (67), suggesting that the Bcl-2 family may control apoptosis through the regulation of intracellular ions. These studies provide further evidence that the regulation of the intracellular ionic environment is a critical mechanism of apoptosis suppression and inappropriate regulation, for example in Bcl-2 overexpression, and may lead to pathological conditions such as cancer.

Finally, it is not clear how intracellular  $K^+$  actually suppresses enzymatic activity, although ionic strength has previously been shown to influence the activity of many different enzymes including proteases (37, 38, 40, 43) and nucleases (39, 41). Ionic strength can affect various aspects of protein structure and function, including interactions with other proteins and the degree of denaturation (68–70). Thus, it is possible that high intracellular  $K^+$  promotes the interaction of apoptotic enzymes with natural inhibitors and/or prevents their interaction with effectors of their activity.  $K^+$  loss may also promote a conformational change in the enzymes that allows for activation in response to an apoptotic signal. Future studies will undoubtedly shed light on the nature of ionic interference with apoptotic enzyme activity.

**Acknowledgments**—We thank Laura Thompson at the Research Triangle Institute for gracious help in measuring intracellular  $K^+$  levels. We also thank Mike Cook and Alan Fisher at Duke University Cancer Center's Flow Cytometry Facility for their expert help in flow cytometry.

#### REFERENCES

- Ellis, H. M., and Horvitz, H. R. (1986) *Cell* **44**, 817–829
- Horvitz, H. R., Shaham, S., and Hengartner, M. O. (1994) *Cold Spring Harbor Symp. Quant. Biol.* **59**, 377–385
- Hengartner, M. O., and Horvitz, H. R. (1994) *Curr. Opin. Gen. & Dev.* **4**, 581–586
- Jacobson, M. D., Weil, M., and Raff, M. C. (1997) *Cell* **88**, 347–354
- Bortner, C. D., and Cidlowski, J. A. (1996) *Am. J. Physiol.* **271**, C950–C961
- Caron-Leslie, L.-A. M., and Cidlowski, J. A. (1994) *Endocr. J.* **2**, 47–52
- Chow, S. C., Peters, I., and Orrenius, S. (1995) *Exp. Cell Res.* **216**, 149–159
- Cotter, T. G., Lennon, S. V., Glynn, J. G., and Martin, S. J. (1990) *Anticancer Res.* **10**, 1153–1160
- Martin, S. J., Bonham, A. M., and Cotter, T. G. (1990) *Biochem. Soc. Trans.* **18**, 634–636
- Alnemri, E. S., Livingston, D. J., Nicholson, D. W., Salvesen, G., Thornberry, N. A., Wong, W. W., and Yuan, J. (1996) *Cell* **87**, 171
- Nagata, S. (1997) *Cell* **88**, 355–365
- Henkart, P. A. (1996) *Immunity* **4**, 195–201
- Patel, T., Gores, G. J., and Kaufmann, S. H. (1996) *FASEB J.* **10**, 587–97
- Whyte, M. (1996) *Trends Cell Biol.* **6**, 245–248
- Kumar, S. (1995) *Trends Biochem. Sci.* **20**, 198–202
- Martin, S. J., and Green, D. R. (1995) *Cell* **82**, 349–352
- Kumar, S., and Lavin, M. F. (1996) *Cell Death Differ.* **3**, 255–268
- Kayalar, C., Ord, T., Testa, M. P., Zhong, L. T., and Bredesen, D. E. (1996) *Proc. Natl. Acad. Sci. U. S. A.* **93**, 2234–2238
- Martin, S. J., O'Brien, G. A., Nishioka, W. K., McGahon, A. J., Mahboubi, A., Saïdo, T. C., and Green, D. R. (1995) *J. Biol. Chem.* **270**, 6425–6428
- Ucker, D. S., Obermiller, P. S., Eckhart, W., Apgar, J. R., Berger, N. A., and Meyers, J. (1992) *Mol. Cell. Biol.* **12**, 3060–3069
- Oberhammer, F. S., Hochegger, K., Froschl, G., Tiefenbacher, R., and Pavelka, M. (1994) *J. Cell Biol.* **126**, 827–837
- Kaufmann, S. H. (1989) *Cancer Res.* **49**, 5870–5878
- Lazebnick, Y. A., Takahashi, A., Moir, R. D., Goldman, R. D., Poirier, G. G., Kaufmann, S. H., and Earnshaw, W. C. (1995) *Proc. Natl. Acad. Sci. U. S. A.* **92**, 9042–9046
- Kaufmann, S. H., Desnoyers, S., Ottaviano, Y., Davidson, N. E., and Poirier, G. G. (1993) *Cancer Res.* **53**, 3976–3985
- Caciola-Rosen, L. A., Anhalt, G. J., and Rosen, A. (1995) *J. Exp. Med.* **182**, 1625–1634
- Compton, M. M., and Cidlowski, J. A. (1987) *J. Biol. Chem.* **262**, 8288–8292
- Montague, J. W., Hughes, F. M., Jr., and Cidlowski, J. A. (1997) *J. Biol. Chem.* **272**, 6677–6684
- Gaido, M. L., and Cidlowski, J. A. (1991) *J. Biol. Chem.* **266**, 18580–18585
- Hughes, F. M., Jr., and Cidlowski, J. A. (1997) *Cell Death Differ.* **4**, 200–208
- Peitsch, M. C., Polzar, B., Stephan, H., Crompton, T., MacDonald, H. R., Mannherz, H. G., and Tschopp, J. (1993) *EMBO J.* **12**, 371–377
- Barry, M. A., and Eastman, A. (1993) *Arch. Biochem. Biophys.* **300**, 440–450
- Wyllie, A. H. (1980) *Nature* **284**, 555–556
- Skalka, M., Matyášová, J., and Čejková, M. (1976) *FEBS Lett.* **72**, 271–274
- Benson, R. S. P., Heer, S., Dive, C., and Watson, A. J. M. (1996) *Am. J. Physiol.* **270**, C1190–C1203
- Barbiero, G., Duranti, F., Bonelli, G., Amenta, J. S., and Baccino, F. M. (1995) *Exp. Cell Res.* **217**, 410–418
- Beauvais, F., Michel, L., and Dubertret, L. (1995) *J. Leukocyte Biol.* **57**, 851–855
- Polgar, L., and Pathy, A. (1992) *Biochemistry* **31**, 10769–10773
- Polgar, L. (1995) *Biochem. J.* **312**, 267–271
- Strickland, J. A., Marzilli, L. G., Puckett, J. M. J., and Doetsch, P. W. (1991) *Biochemistry* **30**, 9749–9756
- Adamska, I., Lindahl, M., Roobol-Boza, M., and Andersson, B. (1996) *Eur. J. Biochem.* **236**, 591–599
- Vukelic, B., Ritonja, A., and Vitale, L. (1995) *Appl. Microbiol. Biotechnol.* **43**, 1056–1060
- Di-Paolo, M. L. (1995) *Arch. Biochem. Biophys.* **323**, 329–334
- Wondrak, E. M., Louis, J. M., and Oroszlan, S. (1991) *FEBS Lett.* **280**, 344–346
- Cidlowski, J. A. (1982) *Endocrinology* **111**, 184–190
- Schwartzman, R. A., and Cidlowski, J. A. (1991) *Endocrinology* **128**, 1190–1197
- Schwartzman, R. A., and Cidlowski, J. A. (1993) *Endocrinology* **133**, 591–599
- Hasegawa, J.-I., Kamada, S., Kamiike, W., Shimizu, S., Imazu, T., Matsuda, H., and Tsujimoto, Y. (1996) *Cancer Res.* **56**, 1713–1718
- Fernandes-Alnemri, T., Litwack, G., and Alnemri, E. S. (1995) *Cancer Res.* **55**, 2737–2742
- Bradford, M. M. (1976) *Anal. Biochem.* **72**, 248–254
- Minta, A., and Tsien, R. Y. (1989) *J. Biol. Chem.* **264**, 19449–19457
- Walev, I., Reske, K., Palmer, M., Valeva, A., and Bhakdi, S. (1995) *EMBO J.* **14**, 1607–1614
- Alberts, B., Bray, D., Lewis, J., Raff, M., Roberts, K., and Watson, J. D. (1983) *Molecular Biology of the Cell*, p. 286, Garland Publishing, New York
- Kuida, K., Lippke, J. A., Ku, G., Harding, M. W., Livingston, D. J., Su, M. S.-S., and Flavell, R. A. (1995) *Science* **267**, 2000–2003
- Li, P., Allen, H., Banerjee, S., Franklin, S., Herzog, L., Johnston, C., McDowell, J., Paskind, M., Rodman, L., Salfeld, J., Towne, E., Tracey, D., Wardell, S., Wei, F.-Y., Wong, W., Kamen, R., and Seshadri, T. (1995) *Cell* **80**, 401–411
- Liu, X., Kim, C., Yang, J., Jemmerson, R., and Wang, X. (1996) *Cell* **86**, 147–157
- Hughes, F. M., Jr., and Cidlowski, J. A. (1998) *J. Steroid Biochem. Mol. Biol.*, in press
- Bortner, C. D., Hughes, F. M., Jr., and Cidlowski, J. A. (1997) in *Programmed Cell Death* (Shi, Y.-B., Shi, Y., Scott, D., and Xu, Y., eds) pp. 63–70, Plenum Publishing Corp., New York
- Jonas, D., Walev, I., Berger, T., Liebetrau, M., Palmer, M., and Bhakdi, S. (1994) *Infect. Immun.* **62**, 1304–1312
- Perregaux, D. G., Laliberte, R. E., and Gabel, C. A. (1996) *J. Biol. Chem.* **271**, 29830–29838
- MacKnight, A. D. C., and Leaf, A. (1977) *Physiol. Rev.* **57**, 510–573
- Kregenow, F. M. (1981) *Annu. Rev. Physiol.* **43**, 493–505
- Al-Habori, M. (1994) *Int. J. Biochem.* **26**, 319–334

<sup>2</sup> C. D. Bortner and J. A. Cidlowski, unpublished observations.

63. Sarkadi, B., Cheung, R., Mack, E., Grinstein, S., Gelfand, E. W., and Rothstein, A. (1985) *Am. J. Physiol.* **248**, C480–C487
64. Grinstein, S., Clarke, C., Dupre, A., and Rothstein, A. (1982) *J. Gen. Physiol.* **80**, 801–823
65. Bortner, C. D., Hughes, F. M., Jr., and Cidlowski, J. A. (1997) *J. Biol. Chem.*, in press
66. Muchmore, S. W., Sattler, M., Liang, H., Meadows, R. P., Harlan, J. E., Yoon, H. S., Nettesheim, D., Chang, B. S., Thompson, C. B., Wong, S.-L., Ng, S.-C., and Fesik, S. W. (1996) *Nature* **381**, 335–341
67. Minn, A. J., Vélez, P., Schendel, S. L., Liang, H., Muchmore, S. W., Fesik, S. W., Fill, M., and Thompson, C. B. (1997) *Nature* **385**, 353–357
68. Nall, B. T., and Dill, K. A. (1991) *Conformations and Forces in Protein Folding*, American Association for the Advancement of Science, Washington, D. C.
69. Creighton, T. E. (1983) *Proteins: Structures and Molecular Properties*, W. H. Freeman & Co., New York
70. Dixon, M., and Webb, E. C. (1979) *Enzymes*, Academic Press, New York